

Physics and Modeling of Noise in SiGe HBT Devices and Circuits

Guofu Niu

Alabama Microelectronics Science and Technology Center, Electrical and Computer Engineering Department, 200 Broun Hall, Auburn University, Auburn, AL 36849, USA

Abstract—This paper gives an overview of the physics and modeling of noise in SiGe HBT devices and circuits, including RF broadband noise, low-frequency noise, and oscillator phase noise. The ability to simultaneously achieve high cutoff frequency (f_T), low base resistance (r_b), and high current gain (β) using Si processing underlies the low levels of low frequency $1/f$ noise, RF noise and phase noise of SiGe HBTs. We will show that the phase noise corner frequency in SiGe HBT oscillators is typically much smaller than the $1/f$ corner frequency measured under *dc* biasing.

Keywords—Noise parameters, SiGe HBT, cyclostationary noise, $1/f$ noise, phase noise.

I. INTRODUCTION

One of the major reasons for the success of SiGe HBT as a RF technology is its low noise capability [1]. In modern digital wireless communications, digital data are modulated onto a RF carrier and transmitted to the receiver, which downconverts the RF carrier to base band for demodulation. The low-noise amplifier, typically the first stage of a receiver, must handle as low as -100 dBm signals, thus requiring very low noise figure devices. Frequency translation is often realized by mixing the modulated RF signal with a local oscillator (LO) signal, which is typically the output of a phase lock loop (PLL) based frequency synthesizer. The phase noise (or spectral impurity) of this frequency synthesizer affects the integrity of the mixed-down signal, and limits the selectivity of the receiver. An important concern here is the VCO phase noise that results from upconversion of low-frequency noises in the transistors.

This paper gives an overview of the physics, modeling and circuit implications of RF broadband noise, low-frequency noise, and oscillator phase noise in SiGe HBT RF technology. We will show that the superior low RF noise figure of SiGe HBT lies in its ability to simultaneously achieve high cutoff frequency (f_T), low base resistance (r_b), and high current gain (β). We will then examine the low-frequency $1/f$ noise, and upconversion of various low-frequency noise to oscillator phase noise. We will show that the phase noise corner frequency in SiGe HBT oscillators is typically much smaller than the $1/f$ corner frequency measured under *dc* biasing.

II. RF NOISE

The primary RF noise sources in a SiGe HBT are the noises associated with the *dc* base and collector currents and the thermal noise of the base resistance. We first discuss physics and models of these noise sources.

A. Origin of Shot Noise

The conventional wisdom is that the power spectral density (PSD) of the base and collector current noises are $2qI$ or “shot” like. The standard derivation of the magic $2qI$ shot noise assumes a Poisson stream of an elementary charge q . These charges need to overcome a potential barrier, and thus flow in a completely uncorrelated manner. In a bipolar transistor, the base current shot noise $2qI_B$ results from the flow of base *majority* holes across the EB junction potential barrier. The reason that I_B appears in the base shot noise is that the amount of hole current overcoming the EB barrier is determined by the minority hole current in the emitter, I_B . Similarly, the collector current shot noise results from the flow of emitter majority electrons over the EB junction potential barrier, and has a spectral density of $2qI_C$.

We emphasize here the EB junction origin of the $2qI_C$ shot noise, which is significantly different from the very popular *CB* junction origin of the $2qI_C$ shot noise believed by many [2]. That is, any *dc* current passing through any *pn* junction has shot noise, and thus the collector current passing through the *CB* junction has the $2qI_C$ shot noise. The two explanations lead to the same collector current noise, but different base current noise and base collector current noise correlation, particularly at RF frequencies [3]. The transition of carriers across the collector-base junction, which is usually reverse-biased for low noise amplification, is a drift process. A DC current passing through such a junction alone does not have intrinsic shot noise. The collector current shows shot noise only because the electron current being injected into the collector-base junction from the emitter already has shot noise, as shown in Fig. 1. The $2qI_C$ shot noise we observe at the collector is *transported* from the EB junction.

B. Transport Noise Model

The emitter current shot noise has two parts, one due to electron injection into the base, and the other due to hole current injection into the emitter, both are “shot” like:

$$S_{i_{ne}} = \frac{\langle i_{ne}^2 \rangle}{\Delta f} = 2qI_C, \quad (1)$$

$$S_{i_{pe}} = \frac{\langle i_{pe}^2 \rangle}{\Delta f} = 2qI_B. \quad (2)$$

Further, they are independent:

$$\langle i_{ne} i_{pe}^* \rangle = 0. \quad (3)$$

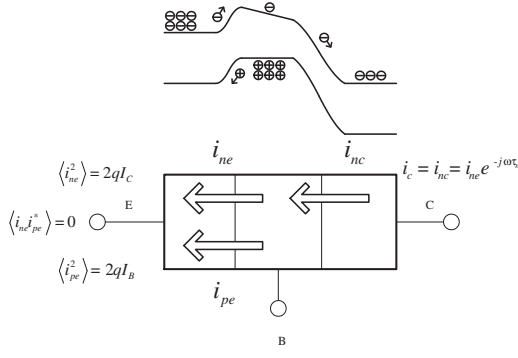


Fig. 1. Illustration of the emitter-base origin of collector current shot noise in a bipolar transistor.

The collector current shot noise is a delayed version of the emitter electron injection induced shot noise:

$$i_c = i_{nc} = i_{ne} e^{-j\omega\tau_n}, \quad (4)$$

where τ_n is the transit time associated with the transport of emitter-injected electron shot noise current, and can be extracted from measured noise data or simulated. We then have:

$$\langle i_c^2 \rangle = \langle i_{nc} i_{nc}^* \rangle = 2qI_C \Delta f, \quad (5)$$

$$\langle i_e^2 \rangle = \langle i_{ne}^2 \rangle + \langle i_{pe}^2 \rangle = 2qI_E \Delta f, \quad (6)$$

$$\langle i_e i_c^* \rangle = 2qI_C e^{j\omega\tau_n} \Delta f. \quad (7)$$

The common-emitter version is:

$$\langle i_b^2 \rangle = \langle i_e^2 \rangle + \langle i_c^2 \rangle - 2 \operatorname{Re} \{ \langle i_e i_c^* \rangle \} \quad (8)$$

$$= [2qI_B + 4qI_C (1 - \operatorname{Re} \{ e^{j\omega\tau_n} \})] \Delta f \quad (9)$$

$$\langle i_c^2 \rangle = 2qI_C \Delta f, \quad (10)$$

$$\langle i_b^* i_c \rangle = \{ \langle i_e i_c^* \rangle \}^* - \langle i_c^2 \rangle \quad (11)$$

$$= 2qI_C (e^{-j\omega\tau_n} - 1) \Delta f \quad (12)$$

The transport shot noise model is also referred to as the unified model, in part because it can be reduced to the conventional SPICE noise model by setting τ_n to zero (or when $\omega \ll 1/\tau_n$). Several recent investigations have shown that this model enables accurate modeling of both experimental noise data and hydrodynamic noise simulation data in SiGe HBTs [3] [4] [5] [6] [7] [8].

Thus far, we have assumed that the base and collector current “shot” noises are caused by majority carriers crossing barriers. Microscopic noise theories, however, show that the $2qI$ shot noise results from the minority carrier velocity fluctuations, with I being the minority carrier current [9] [10] [11]. Velocity fluctuations give rise to current density fluctuations, which then propagate towards the terminals. The collector current shot noise originates from the neutral base, which is close to the physical explanation underlying the transport noise model. This perhaps explains the better accuracy of the transport noise model, as part of the physics is consistent with more fundamental microscopic noise transport. A key issue in microscopic noise simulation of advanced SiGe HBTs is the determination of the local velocity fluctuations under non-equilibrium transport [12] [13].

C. Noise Figure

At circuit level, noise factor F is used as a figure-of-merit, defined as the signal-to-noise ratio at the input divided by the signal-to-noise ratio at the output. Noise figure (NF) defined as $10 \log F$ is often used instead of F .

For a source termination admittance $Y_s = G_s + jB_s$, NF is [14]:

$$NF = NF_{min} + \frac{R_n}{G_s} |Y_s - Y_{s,opt}|^2, \quad (13)$$

where NF_{min} is the minimum noise figure, $Y_{s,opt}$ is the optimum source admittance, and R_n is the noise resistance. Together, they are referred to as the *noise parameters*. Noise figure reaches its minimum when $Y_s = Y_{s,opt}$ or the source is noise matched, while R_n determines the sensitivity of noise figure to deviations from $Y_{s,opt}$. The smallest possible NF_{min} and smaller R_n are obviously desired.

The noise parameters are intrinsic properties of the linear two port, just like the y -parameters or s -parameters. They are functions of the equivalent input noise voltage, current and their correlation. We denote their PSDs as S_{i_n} , S_{v_n} , and $S_{i_n v_n^*}$ below [14].

Under certain assumptions, the equivalent input noise current and voltage can be approximately obtained as:

$$S_{v_n} = 4kTr_b + \frac{2qI_C}{|Y_{21}|^2} + 2qI_B r_b^2, \quad (14)$$

$$S_{i_n} = 2qI_B + \frac{2qI_C}{|H_{21}|^2}, \quad (15)$$

$$S_{i_n v_n^*} = 2qI_C \frac{Y_{11}}{|Y_{21}|^2} + 2qI_B r_b. \quad (16)$$

The Y -parameters and H -parameters have their usual meaning, and can be expressed using equivalent circuit parameters β , I_C , C_{be} , C_{bc} , and $g_m = I_C/v_t$. For a given I_C , a higher β helps in reducing I_B and hence S_{i_n} . A higher f_T helps in increasing H_{21} and hence reducing S_{i_n} . Fundamentally, the inherently high β and high f_T of SiGe HBTs lead to low input noise current. For the same β , the additional bandgap engineering leverage in SiGe HBTs allows one to use higher base doping than in conventional implanted-base Si BJTs, which in turn reduces the input noise voltage.

R_n directly relates to S_{v_n} by:

$$R_n = \frac{S_{v_n}}{4kT} \approx r_b + \frac{1}{2g_m}. \quad (17)$$

A smaller r_b helps in keeping NF close to NF_{min} in cases of noise mismatch. The leverage of bandgap engineering enables a lower r_b in SiGe HBTs than in implanted-base Si BJTs, which translates into a lower sensitivity of noise figure to noise mismatching in addition to a lower NF_{min} . This is highly desirable as noise matching cannot always be achieved due to constraints like power consumption.

The real and imaginary part of $Y_{s,opt}$ are approximately given by [15]:

$$G_{s,opt} = \sqrt{\frac{g_m}{2R_n} \frac{1}{\beta} + \frac{(\omega C_i)^2}{2g_m R_n} \left(1 - \frac{1}{2g_m R_n}\right)}, \quad (18)$$

$$B_{s,opt} = -\frac{\omega C_i}{2g_m R_n}. \quad (19)$$

Here $C_i = C_{be} + C_{bc}$. Eqs. (18) and (19) indicate that the imaginary part of $Y_{s,opt}$ is negative. A series inductor at the base is thus needed for noise matching of the imaginary part. Noting the I_C dependence of C_i (through $g_m = qI_C/kT$), we can further observe that:

- $G_{s,opt}$ increases with I_C in general.
- $G_{s,opt}$ increases with frequency.
- When the diffusion capacitance dominates C_i , $B_{s,opt}$ becomes independent of I_C , as C_i is proportional to g_m .
- The absolute value of $B_{s,opt}$ increases with frequency.

NF_{min} can then be approximately obtained as:

$$NF_{min} = 1 + \frac{1}{\beta} + \sqrt{2g_m r_b} \sqrt{\frac{1}{\beta} + \left(\frac{f}{f_T}\right)^2}. \quad (20)$$

The two terms inside the second square root become equal at $f = f_T/\sqrt{\beta}$, which defines a transition of NF_{min} from a white noise behavior (independent of frequency) to a 10 dB/decade increase as the frequency increases. Eq. (20) also indicates that a low r_b is the key to reducing NF_{min} when $f > f_T/\sqrt{\beta}$.

Fig. 2 shows the NF_{min} , R_n , $G_{s,opt}$ and $B_{s,opt}$ vs frequency for a 60 GHz peak f_T IBM SiGe process. Fig. 3 shows the J_C dependences. The qualitative behavior of all of the noise parameters can be understood using the simplified model equations we described above. Noticeably,

- NF_{min} increases with frequency. For a 52 GHz f_T biasing, NF_{min} is only 3 dB at 25 GHz, which is excellent.
- The NF_{min} at a given frequency has a minimum at a J_C much smaller than the peak $f_T J_C$.
- R_n is weakly frequency dependent. R_n also decreases with J_C at lower J_C , and then stays constant.
- $G_{s,opt}$ increases with frequency and J_C .
- $B_{s,opt}$ is negative, indicating the need to use an inductor for reactive noise matching. $|B_{s,opt}|$ increases with frequency, but is weakly dependent on J_C below 15 GHz.

D. Circuit Design Implications

For circuit design, the SiGe HBT size and biasing current can be optimized. This comes down to optimizing the effective emitter length, as the smallest emitter width of the technology is always used for reducing r_b and NF_{min} . For ideal emitter length scaling,

- NF_{min} is only a function of J_C (or V_{BE}) and independent of emitter length, just like f_T .
- R_n and $Z_{s,opt}$ (inverse of $Y_{s,opt}$), scale with the inverse of emitter length, just like r_b .
- The NF_{min} achievable is a fundamental property of the technology, determined by the device design, and is independent of the emitter length, just like the peak f_T .

These scaling rules generally hold for any devices that are essentially “2-D,” e.g. an ideal bipolar transistor or a CMOS transistor with no gate resistance, and do not rely on specific noise models.

In designing a low-noise amplifier, we first determine the minimum J_C that provides the required f_T or H_{21} . The emitter length of can be scaled so that $R_{s,opt}$ matches the RF source resistance, typically a fixed 50Ω. Tens of microns are often required to noise match such a small resistance by

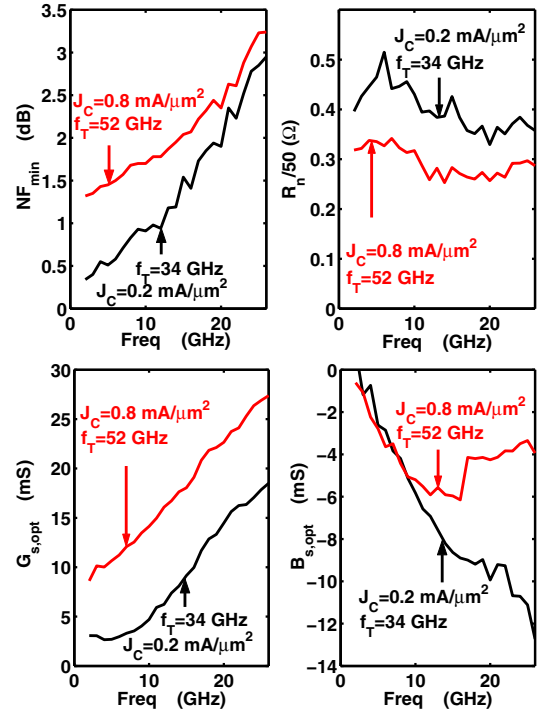


Fig. 2. Noise parameters vs frequency for a SiGe HBT with 60 GHz peak f_T . $A_E = 0.24 \times 10 \times 2 \mu\text{m}^2$.

IC standard. The imaginary part is easily matched using a base inductor. Simultaneous impedance matching and noise matching is achieved using an emitter inductor, which produces an input resistance without much effect on $R_{s,opt}$. The base inductance is adjusted accordingly to ensure simultaneous noise and impedance matching of the imaginary part.

III. LOW-FREQUENCY $1/f$ NOISE

Another type of noise we are concerned with a RF semiconductor technology is low-frequency $1/f$ noise, also known as flicker noise. The value of such noise can be quite high at low frequencies close to dc . $1/f$ noise is thus clearly a concern for low-noise analog circuits that need to operate at low frequencies, e.g. the amplifiers used in a zero intermediate frequency (IF) direct conversion receiver. A less obvious but widely discussed effect is that low-frequency noise can be upconverted to oscillator phase noise, which limits spectral purity and degrades the signal integrity of frequency translations. Generally speaking, both the base current and collector currents have low-frequency noise [16]. However, in most cases, the base current $1/f$ noise dominates.

Fig. 4 shows a typical low-frequency base current noise spectrum (S_{I_B}) for a SiGe HBT. The noise spectrum shows a clear $1/f$ component as well as the $2qI_B$ shot noise level. The corner frequency f_c , a well quoted figure-of-merit for $1/f$ noise, is defined by the intercept of the $1/f$ component and the $2qI_B$ shot noise level. At higher I_B values, the $2qI_B$ shot noise level cannot be directly observed for various reasons. The calculated $2qI_B$ value can be used to determine f_c in this case.

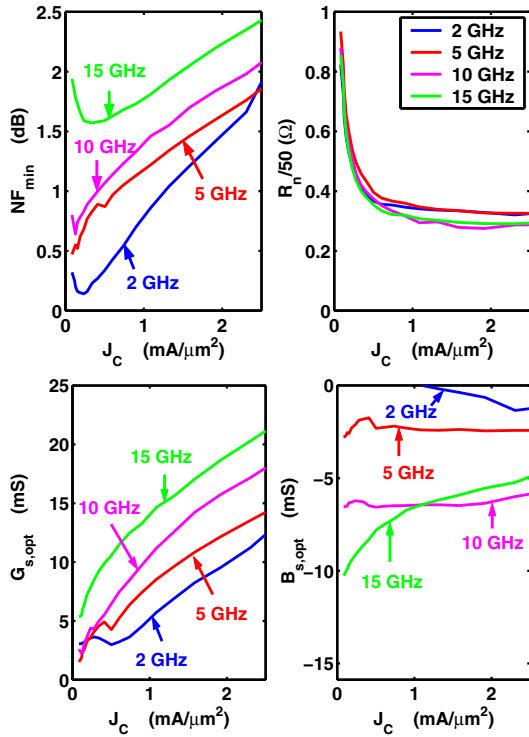


Fig. 3. Noise parameters vs J_C for a 60 GHz peak f_T SiGe HBT. $A_E=0.24 \times 10 \times 2 \mu\text{m}^2$.

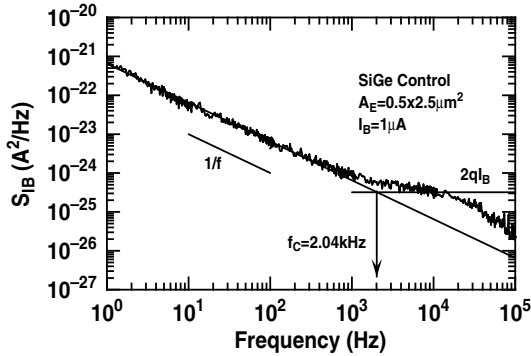


Fig. 4. A typical low-frequency noise spectrum of a first generation SiGe HBT ($A_E = 0.5 \times 2.5 \mu\text{m}^2$, and $I_B = 1 \mu\text{A}$).

A popular theory of $1/f$ noise, proposed by McWhorter [17], describes $1/f$ noise as a superposition of individual generation-recombination (g-r) noise. Each trap generates g-r noise with a Lorentzian shaped PSD. A large number of traps with a particular statistical distribution of the trapping-detrapping time constant τ_i ($1/\tau$) leads to the $1/f$ spectral shape. Tunneling of carriers through an oxide barrier can lead to a $1/\tau$ distribution. Both the polysilicon to crystal silicon interfacial oxide and the oxide spacers around the emitter perimeter could be responsible for $1/f$ noise in SiGe HBTs. Experimental data supports the above trapping origin of $1/f$ noise in SiGe HBTs [18].

A. SiGe Profile Impact

In general, S_{I_B} is related to I_B by

$$S_{I_B} = K_F \frac{I_B^\alpha}{f}, \quad (21)$$

where K_F and α correspond to the KF and AF model parameters used in SPICE. $\alpha = 1$ is often viewed as indication of carrier mobility fluctuations, and $\alpha = 2$ is often viewed as for carrier number fluctuations [19], [20], [21], [22]. The α for typical SiGe HBTs is close to 2, and varies only slightly with SiGe profile and collector doping profile (2 ± 0.2).

Assuming that the $1/f$ noise is only a function of the number of minority carriers injected into the emitter, one may expect the same $1/f$ noise at a given V_{BE} , which means the same I_B for a SiGe HBT and its Si counterpart. Thus, the $1/f$ noise K factor is expected to be the same. This turns out to be true experimentally [23].

For circuit design, a comparison at the same I_C is more meaningful. S_{I_B} is significantly lower (better) in SiGe HBTs than in Si BJTs, because of the lower I_B (higher β) found in SiGe HBTs, all else being equal. Since $S_{I_B} \propto I_C^2/\beta^2$, the S_{I_B} for the LN1 and LN2 SiGe HBTs should be naturally lower than for the SiGe control and Si BJT because of their higher β . This is confirmed by the measured data [23].

B. $1/f$ Corner Frequency

Traditionally, $1/f$ noise performance is characterized by the corner frequency ($f_{c,1/f}$) figure-of-merit, defined to be the frequency at which the $1/f$ noise equals the shot noise level $2qI_B$. Assuming $\alpha = 2$,

$$f_{c,1/f} = \frac{KI_B}{2qA_E} = \frac{KJ_C}{2q\beta}, \quad (22)$$

where $J_C = I_C/A_E$, and $\beta = I_C/I_B$. Thus $f_{c,1/f}$ is proportional to J_C and K , and inversely proportional to β . Fig. 5 shows the measured and modeled $f_{c,1/f} - J_C$ for devices of various SiGe designs. As expected, f_c is the lowest in the two low-noise SiGe HBTs, LN1 and LN2, and highest for the Si BJT.

The above definition of $f_{c,1/f}$ involves only the base current $1/f$ and shot noises, and thus is not a complete indicator of the relative importance of $1/f$ noise with respect to white noise. The $1/f$ corner frequency is not a good indicator of the relative importance of $1/f$ noise and other white noises in determining oscillator phase noise either, due to the different upconversion mechanisms of various noise sources [24].

IV. PHASE NOISE

An important issue for integrated transceiver design is to minimize voltage controlled oscillator (VCO) phase noise, and ultimately frequency synthesizer phase noise. The exact mechanism of phase noise is still an active area of research. The basic behavior of upconversion can be understood as follows using a simplified version of the time domain model proposed in [25] [26]. Consider injecting a unity impulse perturbation current into an oscillator. The resulting amplitude shift dies away due to built-in amplitude limiting mechanisms, while the phase shift remains as any time-shifted

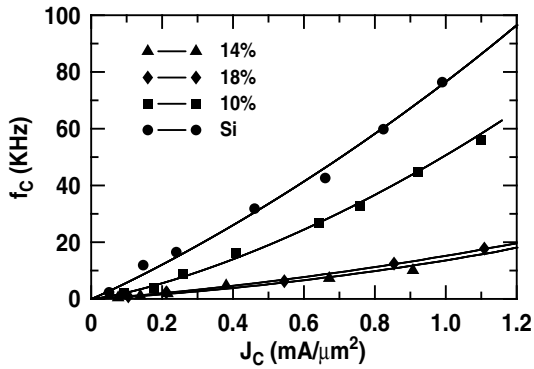


Fig. 5. Measured and modeled $f_{c,1/f}$ versus J_C for the Si BJT, the SiGe control, and the two low-noise SiGe HBTs.

version of the solution remains a solution. The response can be approximated using a step function $s(t)$ as we are not concerned with short term time constants. We further assume that $s(t)$ is independent of the injection time instant for simplicity. For an arbitrary noise u , the accumulated phase shift is:

$$\phi(t) \propto \int_{-\infty}^t u(\tau)s(t-\tau)d\tau \propto \int_{-\infty}^t u(\tau)d\tau, \quad (23)$$

thus the PSD of ϕ is related to the PSD of the physical noise u by:

$$S_\phi \propto \frac{S_u}{(2\pi f)^2}. \quad (24)$$

For white noise such as base resistance thermal noise and shot noise, S_u is white, $S_\phi \propto 1/f^2$. For $1/f$ noise, $S_u \propto 1/f$ and $S_\phi \propto 1/f^3$.

One may attempt to apply this simple theory to transistor base current noise, and conclude that the $1/f^3$ and $1/f^2$ phase noises due to base $1/f$ and shot noise will intersect at an offset equal to the $1/f$ corner frequency. This cannot be farther from the truth, primarily because of the large signal operating nature of transistor oscillators, which makes the phase noise upconversion process much more complicated to analyze.

We now examine the phase noise behavior in SiGe HBT oscillators using ADS simulation. 5.5 GHz Colpits oscillators are designed and phase noise are simulated for a 50 GHz HBT and a 120 GHz HBT. We chose two HBTs of similar emitter area from the two processes, as $1/f$ noise is inversely proportional to emitter area.

A. Noise Generating Current in Oscillators

So far we have considered small signal linear $1/f$ noise measured under a given biasing I_B . Oscillators, however, are large signal and nonlinear in nature. The physical noise behavior is more complicated as [24]:

- Terminal I_B is different from the base-emitter junction transport current I_{BE} , because of the capacitive current. Only I_{BE} generates noise.
- The noise generating I_{BE} is “oscillating” by the very nature of oscillation.

Fig. 6 compares terminal I_B and internal noise generating I_{BE} in a 5.5 GHz SiGe HBT oscillator. Also shown is the

V_{BE} waveform. Clearly, a large difference exists between I_{BE} and I_B .

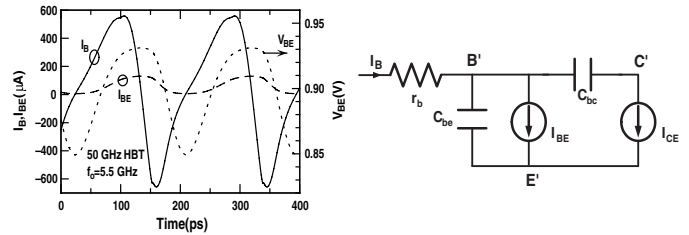


Fig. 6. Comparison of terminal I_B and internal I_{BE} for a SiGe HBT in an oscillator.

In circuit simulators such as ADS and SpectreRF, the amount of $1/f$ noise for an oscillating transistor is assumed to be the same as the $1/f$ measured at a dc biasing current identical to the dc component of the oscillating noise generating current I_{BE} .

B. Phase Noise Corner Frequency

Fig. 7 shows simulated phase noise versus offset frequency for two HBTs with 50 and 120 GHz peak f_T . With device scaling, the $1/f^3$ component increases by 11.4 dB, in part because of the increasing K factor. The $1/f^2$ phase noise, however, improves (decreases) by 7.2 dB, primarily due to base resistance reduction. We can define the corner offset frequency, $f_{c,offset}$, using the intersect of the $1/f^3$ and $1/f^2$ phase noises. $f_{c,offset}$ is a direct measure of the importance of the phase noise upconverted from $1/f$ noise with respect to the phase noise upconverted from the white noise sources. $f_{c,offset}$ is 595.4 Hz and 40.8 kHz for the 50 and 120 GHz HBTs. $f_{c,offset}$ itself does not contain any information on either the $1/f^3$ or $1/f^2$ phase noise level. Its utility is that it defines the transition from $1/f^3$ to $1/f^2$ dependence. Perhaps surprisingly, these phase noise corner frequencies are much smaller than the $1/f$ corner frequencies at the biasing currents (200 kHz and 1.4 MHz). This observation is typically true for bipolar oscillators for various reasons [24].

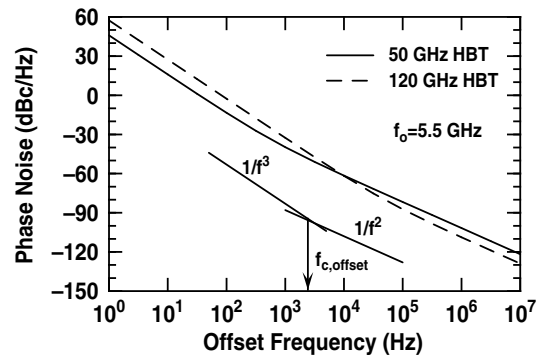


Fig. 7. Phase noise of oscillators designed using HBTs with 50 and 120 GHz peak f_T .

A higher $f_{c,offset}$ does not necessarily mean higher phase noise. In the case discussed above, the $f_{c,offset}$ for the 120

GHz HBT is nearly $70\times$ higher than for the 50 GHz HBT (Fig. 7). The overall effect of scaling is a degradation at offsets below 10 kHz, but an improvement at higher offset frequencies. In a frequency synthesizer, if the loop bandwidth is much greater than 10 kHz, the overall synthesizer phase noise will improve with scaling, despite increased $1/f$ corner frequency, as the oscillator phase noise below 10 kHz is removed by loop feedback.

V. SUMMARY

We have discussed the physics, modeling and circuit implications of low-frequency noise, RF noise and phase noise in SiGe HBT RF technologies. The ability to simultaneously achieve high cutoff frequency (f_T), low base resistance (r_b), and high current gain (β) using Si processing underlies the low levels of low-frequency $1/f$ noise, RF noise and phase noise of SiGe HBTs. The relative importance of $1/f$ noise induced $1/f^3$ phase noise with respect to white noise induced $1/f^2$ phase noise is much less than what the $1/f$ corner frequency may indicate. SiGe HBTs with high corner frequency can still show excellent phase noise performance when used in oscillators.

ACKNOWLEDGMENTS

This work was supported by SRC under #2003-NJ-1133, and NSF under ECS #0112923 and #0119623. The author would like to thank J. Tang, Y. Cui, K. Xia, Z. Feng, D. Sheridan, S. Sweeny, A. Joseph, D. Harame, Q. Liang, Z. Jin, J. Cressler, and the IBM SiGe team for their contributions.

REFERENCES

- [1] J. Cressler and G. Niu, *Silicon-Germanium Heterojunction Junction Bipolar Transistors*. Artech House, 2003.
- [2] A. van der Ziel, "Theory of shot noise in junction diodes and junction transistors," *Proc. IRE*, vol. 43, pp. 1639–1646, Nov. 1955.
- [3] G. Niu, J. Cressler, W. Ansley, C. Webster, and D. Harame, "A unified approach to RF and microwave noise parameter modeling in bipolar transistors," *IEEE Transactions on Electron Devices*, vol. 48, pp. 2568–2574, Nov. 2001.
- [4] J. Moller, B. Heinemann, and F. Herzel, "An improved model for high-frequency noise in BJTs and HBTs interpolating between the quasi-thermal approach and the correlated-shot-noise model," in *Proceedings of the IEEE BCTM*, pp. 228 – 231, 2002.
- [5] P. Sakalas, M. Schroter, P. Zampardi, H. Zirath, and R. Welse, "An improved model for high-frequency noise in BJTs and HBTs interpolating between the quasi-thermal approach and the correlated-shot-noise model," in *IEEE MTT-S International Microwave Symposium Digest*, pp. 2117 – 2120, 2002.
- [6] P. Sakalas, M. Schroter, R. Scholz, H. Jiang, and M. Racanelli, "Analysis of microwave noise sources in 140 GHz SiGe HBTs," in *IEEE RFIC Digest*, pp. 291 – 294, 2004.
- [7] G. Niu, K. Xia, D. Sheridan, and D. Harame, "Experimental extraction and model evaluation of base and collector current RF noise in SiGe HBTs," in *IEEE RFIC Digest*, pp. 615 – 618, 2004.
- [8] C. Jungemann, B. Neinhuis, B. Meinerzhagen, and R. Dutton, "Investigation of compact models for RF noise in SiGe HBTs by hydrodynamic device simulation," *IEEE Transactions on Electron Devices*, vol. 51, pp. 956–961, June 2004.
- [9] K. M. van Vliet, "General transistor theory of noise in PN junction-like devices—i. three-dimensional green's function formulation," *Solid-State Electronics*, vol. 15, pp. 1033–1053, Oct. 1972.
- [10] Y. Cui, G. Niu, and D. Harame, "An examination of bipolar transistor noise modeling and noise physics using microscopic noise simulation," in *Proceedings of the IEEE BCTM*, pp. 183–186, 2003.
- [11] G. Niu, "Bridging the gap between microscopic and macroscopic theories of noise in bipolar junction transistors," in *Tech. Digest of IEEE NSTI-Nanotech 2005*, www.nsti.org, ISBN 0-9767985-3-0 WCM, 2005.
- [12] C. Jungemann, B. Neinhuis, and B. Meinerzhagen, "Hierarchical 2-d DD and HD noise simulations of Si and SiGe Devices – part i: Theory," *IEEE Transactions on Electron Devices*, vol. 49, pp. 1250–1257, July 2002.
- [13] C. Jungemann, B. Neinhuis, and B. Meinerzhagen, "Hierarchical 2-d DD and HD noise simulations of Si and SiGe devices – part ii: Results," *IEEE Transactions on Electron Devices*, vol. 49, pp. 1258–1264, July 2002.
- [14] Haus *et al.*, "Representation of noise in linear twoports," *Proc. IRE*, vol. 48, pp. 69–74, 1960.
- [15] G. Niu and J. Cressler, "Noise-gain tradeoff in RF SiGe HBTs," *Solid-State Elect.*, vol. 46, pp. 1445–1451, 2002.
- [16] L. Bary, G. Cibiel, J. Ibarra, *et al.*, "Low frequency noise and phase noise behavior of advanced SiGe HBTs," in *Tech. Digest of IEEE RFIC Symposium*, May 2001.
- [17] A. McWhorter, *Semiconductor Surface Physics*. 1980.
- [18] Z. Jin, J. Cressler, G. Niu, and A. Joseph, " $1/f$ noise sources," *Impact of Geometrical Scaling on Low-frequency Noise in SiGe HBTs*, vol. 50, pp. 676–682, Mar. 2003.
- [19] L. Vandamme, "Noise as a diagnostic tool for quality and reliability of electronic devices," *IEEE Trans. Elect. Dev.*, vol. 41, pp. 2174–2187, Nov. 1994.
- [20] M. Deen, J. Ilowski, and P. Yang, "Low frequency noise in polysilicon-emitter bipolar junction transistors," *J. Appl. Phys.*, vol. 77, pp. 6278–6285, 1995.
- [21] P. Llinares, D. Celi, and O. R. dit Buisson, "Dimensional scaling of $1/f$ noise in the base current of quasi self-aligned polysilicon emitter bipolar junction transistors," *J. Appl. Phys.*, vol. 82, pp. 2671–2675, 1997.
- [22] M. Deen, S. Romyantsev, and M. Schroter, "On the origin of $1/f$ noise in polysilicon emitter bipolar transistors," *J. Appl. Phys.*, vol. 85, pp. 1192–1195, 1999.
- [23] G. Niu, Z. Jin, J. Cressler, R. Rapeta, A. Joseph, , and D. Harame, "Transistor noise in SiGe HBT RF technology," *IEEE Journal of Solid-State Circuits*, vol. 36, pp. 1424–1427, 2001.
- [24] G. Niu, J. Tang, Z. Feng, A. Joseph, and D. Harame, "Scaling and technological limitations of $1/f$ noise and oscillator phase noise in SiGe HBTs," *IEEE Trans. Micro. Theory Tech.*, vol. 53, pp. 506–514, Feb. 2005.
- [25] A. Hajimiri and T. H. Lee, "A general theory of phase noise in electrical oscillators," *IEEE J. Solid-State Circuits*, vol. 33, pp. 179–194, Feb. 1998.
- [26] K. Kundert, "Introduction to rf simulation and its application," *IEEE J. Solid-State Circuits*, vol. 34, pp. 1298–1319, Sept. 1999.